Morris, J.D., Villinger, H.W., and Klaus, A. (Eds.)
Proceedings of the Ocean Drilling Program, Scientific Results Volume 205

14. Calcareous Nannofossil Biostratigraphy: Ocean Drilling Program Leg 205, Costa Rica Subduction Zone[1]

Jay P. Muza[2]

ABSTRACT

Ocean Drilling Program Leg 205 of the research vessel *JOIDES Resolution* was a return expedition to the Leg 170 sites located on the Costa Rica subduction zone. Here the entire sediment cover on the incoming Cocos plate, including significantly large sections of calcareous nannofossil ooze and chalk, is underthrust beneath the overriding Caribbean plate. The large amount of subducted carbonate produces characteristic styles of volcanic and seismic activity that differ from those found farther along strike in Nicaragua and elsewhere. An understanding of the fate of subducted carbonate sediment sections is an essential component to our understanding of the global biogeochemical cycling of carbon dioxide. Because Leg 205 drilling operations were performed within meters of the Leg 170 drill sites occupied during October–December 1996, minimal coring was done during Leg 205. Although the biostratigraphy of the Leg 170 sites has since been documented in detail, questions remained regarding the age and nature of a gabbro sill that was only partially penetrated by coring during Leg 170. Coring operations during Leg 205 fully penetrated the gabbro sill, followed by an additional 12 m of sediments below the sill, and then ~160 m of gabbro. Coring halted at 600 meters below seafloor (mbsf). Calcareous nannofossil age dating of the sediments immediately above the igneous sill, as well as the sediment between the sill and the lower igneous unit, indicates a minimum age of 15.6 Ma and a maximum age of 18.2 Ma for the sediments. This implies that the sill was emplaced more recently

[1]Muza, J.P., 2006. Calcareous nannofossil biostratigraphy: Ocean Drilling Program Leg 205, Costa Rica subduction zone. *In* Morris, J.D., Villinger, H.W., and Klaus, A. (Eds.), *Proc. ODP, Sci. Results,* 205, 1–26 [Online]. Available from World Wide Web: <http://www-odp.tamu.edu/publications/205_SR/VOLUME/CHAPTERS/211.PDF>. [Cited YYYY-MM-DD]
[2]Department of Physical Sciences (Oceanography and Geology), Broward Community College, 3501 Southwest Davie Road, Fort Lauderdale FL 33314, USA.
jmuza@broward.edu

Initial receipt: 3 May 2005
Acceptance: 10 November 2005
Web publication: 3 May 2006
Ms 205SR-211

than 18.2 Ma. The calcareous nannofossil assemblage in baked sediments in contact with the top of the lower igneous unit also suggests that the maximum age for emplacement is 18.2 Ma.

At Site 1254, coring was accomplished between 150 and 230 mbsf (prism section), and from 300 to 367.5 mbsf (prism and through the décollement into the underthrust section). In the interval from 150 to 322 mbsf, the biostratigraphic analysis of calcareous nannofossils suggests that the sediments are early Pleistocene age between 150 and 161 mbsf, late Pliocene age from 161 to 219 mbsf, and early Pliocene age from 219 to 222 mbsf (no younger than 3.75 Ma). The lack of marker fossils in the interval of sediments cored from 300 to 350.6 mbsf does not allow for any age determinations; however, sediments from 351.6 to 359.81 mbsf could be age dated and are also early Pliocene age, but no younger than 3.75 Ma.

At Site 1255, limited coring was accomplished only in the décollement because of time constraints. Sediments cored at this site are tentatively dated as middle to late Pleistocene.

INTRODUCTION

Beginning with Ocean Drilling Program Leg 170, a comprehensive investigation was undertaken to arrive at an understanding of the fate of subducted materials at the "Costa Rica subduction factory." See Figure **F1** for a regional view of the study area that shipboard researchers have called the Costa Rica subduction factory and the location of the Leg 205 transect across the Middle America Trench. During Leg 170, and the subsequent years leading up to Leg 205, shipboard and shore-based researchers were successful in characterizing the lithologic, chemical, and stratigraphic nature of both the underthrust section and overriding plate at Leg 170 Sites 1039, 1040, 1041, 1042, and 1043. This new understanding led to plans to return to the Leg 170 drill sites for further exploration and sampling. Scientists returned during Leg 205 to install long-term borehole observatories to sample fluids, monitor pressure and temperature, and analyze gas compositions in the underthrust igneous section and overriding sedimentary section. To this end, Sites 1253, 1254, and 1255 were drilled and partially cored within the study area during Leg 205. Coring objectives, including age dating of the lithology at Sites 1253, 1254, and 1255, were successful. Borehole observatories were successfully emplaced at Sites 1253 and 1255.

Other targets of exploration were to focus on the nature of the décollement at Site 1254 located on the overriding plate, as well as a fault zone within the prism sediments at Site 1254 first discovered during Leg 170 at Site 1040. At Site 1253, the primary focus was to investigate the origin, extent, petrology, and tectonic history of the subducting gabbro sill first observed during Leg 170 at Site 1039 and a massive lower gabbro section cored during Leg 205. At Site 1255, very limited coring was conducted because the only major objective at this site was to install a borehole observatory and because of timing constraints. Sites 1039, 1040, and 1043 were used as reference sites for Sites 1253, 1254, and 1255, respectively. Figure **F2** shows the locations of Sites 1039 and 1253 on underthrust Cocos plate, Sites 1255 and 1043 near the toe of the wedge of the overlying prism, and Sites 1254 and 1040, farther from the deformation front than Sites 1255 and 1043. A more detailed bathymetric map of the immediate Leg 205 operations area, with both Leg 205 and Leg 170 site locations is shown in Figure **F3.**

F1. Bathymetry and topography, p. 13.

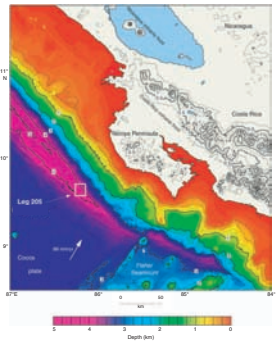

F2. Site locations, p. 14.

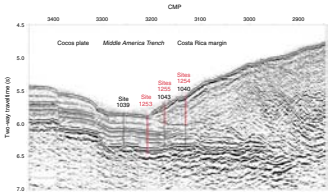

F3. Area of operations, p. 15.

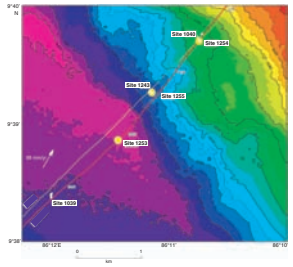

PURPOSE

The purpose of this study was to provide age vs. depth relationship data, utilizing calcareous nannofossils for age determination, for all of the cores recovered during Leg 205. The Leg 205 scientific party had indicated a particular need for biostratigraphic data to help answer several important questions regarding age determinations of the cored sediments and, by association, several igneous units (Morris, Villinger, Klaus, et al., 2003).

Coring at Site 1253 penetrated an upper gabbro sill as well as a lower igneous section (Fig. F4). The upper gabbro sill is correlated to the gabbro sill encountered at Site 1039. The deeper, lower igneous section was not penetrated at Site 1039. Nannofossil chalk was recovered between the upper sill and the lower igneous gabbro. Biostratigraphy from Site 1039 indicated that the upper gabbro sill is between 15.6 and 18.2 m.y. old. Analysis of the seafloor magnetic anomalies on the incoming Cocos plate indicates that the oceanic crust at Sites 1039 and 1253 was produced at the East Pacific Rise at ~24 Ma (Barckhausen et al., 2001). At Site 844, some 400 mi west of Site 1253 and 1039, the ocean basement age is 15 to 17 Ma. Based on Site 844 chronology, an extrapolation using average East Pacific Rise spreading rates indicates that the basement age at Sites 1039 and 1253 might be as old as 21- to 25-Ma age.

Thus, age dating of the chalk is important in ascertaining the structural nature and origin of the lower igneous unit (multiple sills, thickly layered lava flows, or other recognizable oceanic basement). If the nannofossils indicate a possible 21–25 Ma age for the chalk, then there is support for the lower igneous unit being oceanic basement rather than a sill complex. The age determination of the upper igneous unit, the gabbro sill at Site 1039, is confirmed in this study.

Also of great interest is the nature of the décollement, cored at Sites 1254 and 1255, and Sites 1040 and 1043 (Figs. F5, F6). At both Sites 1254 and 1040, the top of the décollement lies within the massive silty clay/claystone with bedded sands characteristic of the hemipelagic prism sediments present at both sites (Morris, Villinger, Klaus, et al., 2003). The base of the décollement, however, differs in character at each site. At Site 1040, the base of the décollement coincides with the lithologic boundary between the upper prism sediments and the underlying underthrust section (Fig. F5). At Site 1254, the base of the décollement has apparently "cut down" into clayey diatomite that composes the uppermost underthrust section at both Sites1254 and 1040. Shipboard scientists have indicated that it would be very useful to know the age of the incoming sediments above and below the décollement boundaries (Morris, Villinger, Klaus, et al., 2003).

Furthermore, age dating of the prism sediments at Site 1040 was hindered by a low abundance of nannofossils, lack of clear grading or bedding, mixing, and reworking of Pliocene through middle Miocene nannofossils among the mostly reworked Pleistocene assemblages (Muza, 2000). Biostratigraphic analysis of the additional samples from Site 1254, along with the Site 1040 biostratigraphic data, may help in defining a more precise age for the lower part of the prism section, which is crucial in helping to determine the nature of the décollement. A higher resolution composite biostratigraphy may also be possible for other intervals within the prism section. Resolution of the biostratigraphic record for the sedimentary prism may provide the ages for

F4. Stratigraphic profile, Hole 1253A, p. 16.

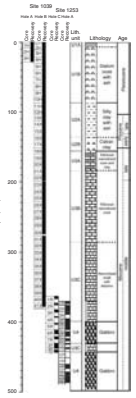

F5. Stratigraphic profile, Hole 1254A, p. 17.

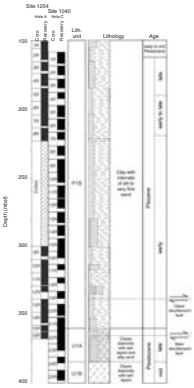

F6. Stratigraphic profile, Hole 1255A, p. 18.

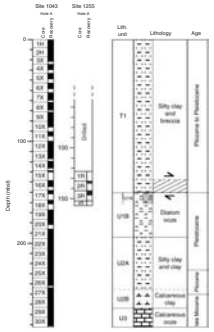

some of the more interesting individual lithologies within the prism. Since it is expected that comparisons will be made between the research accomplished by Muza (2000) and this study, this paper has been written to make those comparisons easier.

METHODS

A total of 133 samples (~1 sample per core section sampling density) were taken from the split core surfaces aboard the *JOIDES Resolution* for calcareous nannofossil biostratigraphic analysis. In a shore-based laboratory, these samples were processed to separate the clay-sized nannofossil fraction from the rest of the sediments by suspending the raw sediment in water and then transferring the clay-sized portion to a coverslip using a pipette. The material on the coverslip was dried, and the coverslip was cemented to a glass microscope slide using Norland optical adhesive #61 and cured under ultraviolet light. Processing the samples in this manner evenly distributes the nannofossils on a microscope slide, resulting in a higher confidence level of reproducibility in quantitative or semiquantitative analyses. All samples were observed and analyzed under phase-contrast and cross-polarized light at magnifications of 400× and 1000×. The diameter of the field of view at 1000× is ~0.21 mm. The observed area in one field of view is ~0.329 mm² at 1000× magnification.

Calcareous nannofossil range distribution charts were constructed for all nannofossil species observed in each hole cored at Sites 1253, 1254, and 1255. The distribution, relative abundance, and relative preservation of nannofossil species or genera observed in the cores at these sites are plotted on Tables **T1, T2,** and **T3.** A logarithmic scale is used to express species or genera abundance. The difference between corresponding abundances in the scale translate into a tenfold increase or decrease in the average number of species seen in 100 or more fields of view on a slide at a magnification of 1000×. Abundances are coded as letters and defined as follows:

H = highly abundant (>100 specimens per field of view [FOV]),
V = very abundant (11–100 specimens per FOV),
A = abundant (1–10 specimens per FOV),
C = common (1 specimen per 2–10 FOV),
F = few (1 specimen per 11–100 FOV), and
R = rare (1 specimen per 101–1000 FOV).

For this study, *Sphenolithus abies*, *Sphenolithus neoabies*, and *Sphenolithus moriformis* were grouped together and appear in the range and distribution tables as undifferentiated *Sphenolithus abies/neoabies/moriformis*. Likewise, *Reticulofenestra minuta, Reticulofenestra minutula,* and *Reticulofenestra haqii* have been grouped together and appear in the range and distribution tables as undifferentiated *Reticulofenestra minuta/minutula/haqii*.

The state of preservation of the fossils is determined by qualitatively ascertaining the overall preservation of the assemblage, even though the state of preservation between different species may vary. Through visual inspection at 1000× the following basic criteria were used to qualitatively describe the degree of preservation, dissolution, or overgrowth of a nannofossil assemblage:

T1. Nannofossils, Hole 1253A, p. 22.

T2. Nannofossils, Hole 1254A, p. 23.

T3. Nannofossils, Hole 1255A, p. 25.

G = good (individual specimens exhibit no dissolution or recrystallization),
M = moderate (individual specimens yield slight evidence of recrystallization or dissolution; no difficulty in determining the species level), and
P = poor (individual specimens exhibit considerable dissolution, recrystallization, and/or overgrowth; species identification is difficult or impossible; identification even at the generic level may be difficult).

Descriptions of species noted in this study and their references can be found in Perch-Nielsen (1985). A list of species considered or noted in this study can be found in the "Appendix," p. 12.

STRATIGRAPHIC STANDARDS

Where applicable, the standard calcareous nannoplankton zones of Martini (1971), Bukry (1973, 1975), and Okada and Bukry (1980) have been considered or determined for the calcareous nannofossil distribution recorded from the Leg 205 cores (Tables T1, T2, T3). The comprehensive correlation between the nannofossil zones of Martini (1971) and Bukry (1973, 1975) and the astronomical/geomagnetically derived chronologic scale of Berggren et al. (1995a, 1995b) used in this study is shown in Figure F7 for the Pleistocene and Pliocene and Figure F8 for the Miocene.

Cores are biostratigraphically analyzed by working from the top of the cored sequence to the bottom of the sequence, also called working "downsection." The first sighting of a species while working downsection is referred to as the "top" of the species range. While continuing to work downsection, the last sighting of the species is considered its "bottom." In all of the cored intervals, it is unknown whether the bottom of a species range actually represents that time when that species was newly introduced globally or that the top of the species range in the section represents that time immediately before the species went globally extinct. It is important to keep these definitions of a particular species' top and bottom in mind when relying on correlation to absolute ages, since the observed tops and bottoms may not actually represent the global introduction of new species or global species extinction. This caveat is especially important to consider when working with sporadic occurrences, sparse species abundances, and sedimentation modes characteristic of debris flow deposits, as observed in all the prism sediments at Leg 205 and 170 sites. Globally derived standard ages of calcareous nannofossil tops and bottoms of marker species used in this study and the author's Leg 170 study are outlined in Table T4 (Muza, 2000).

CALCAREOUS NANNOFOSSIL BIOSTRATIGRAPHIC SYNTHESIS

A synthesis of the occurrence of calcareous nannofossils recovered from the cored sequences at Sites 1253, 1245, and 1255 is presented. Because the primary purpose of the nannofossil analyses at all the Leg 205 sites is to establish a geologic age-depth relationship for the sediments cored at each site, most of the nannofossil analyses center on the loca-

F7. Pleistocene and Pliocene timescale, p. 19.

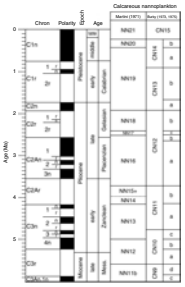

F8. Miocene timescale, p. 20.

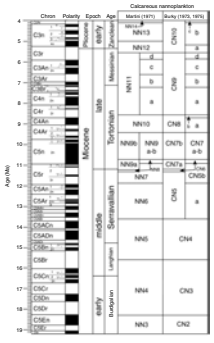

T4. Age ranges, p. 26.

tion of the top and bottom of the ranges of index nannofossil species in the cores and assigning nannofossil zones to the cored sequences where possible.

Nannofossil Distribution, Abundance, Preservation, and Chronology

Site 1253

The distribution, abundance, and preservation of calcareous nannofossils recovered from Hole 1253A, correlated to the nannofossil zonation scheme of Martini (1971) and the chronologic scale of Berggren et al. (1995a, 1995b), is presented in Table T1.

Site 1253 is located ~1.4 km west of Site 1039 on the Cocos plate. The stratigraphy of the cored sequence at Site 1253 (Fig. F4) very closely matches the stratigraphy at the same level in cores from Site 1039 (Morris, Villinger, Klaus, et al., 2003). One of the primary goals at this site was to recore the sediments directly above the sill encountered at Site 1039, core the sediments below the sill to obtain age dates, and core the lower igneous rock unit to ascertain its nature and extent.

After drilling and washing to a depth of 370 meters below seafloor (mbsf), sediment coring was initiated into a sequence of nannofossil chalks interbedded with minor clay layers. Continued coring through the sedimentary sequence reached the upper gabbro sill at 400 mbsf. Coring continued through the sill, reaching the bottom of the sill at ~431 mbsf (the same sill encountered at Site 1039), as well as a thick lower igneous section. Coring was maintained through a ~12-m carbonate sedimentary sequence that separated the upper gabbro sill and a much larger lower gabbro unit. The lower gabbro unit was cored to a depth of ~600 mbsf, where coring terminated (Morris, Villinger, Klaus, et al., 2003).

Approximately one sample per cored sediment section was biostratigraphically analyzed. High abundances and good preservation are characteristic of all of the calcareous nannofossil assemblages, with the exception of five samples taken within ~1 m from the top of the upper sill intrusion and ~0.5 m below the intrusion. Five samples taken nearest the intrusion are barren or consist of highly recrystallized, nannofossil-sized carbonate grains.

Sphenolithus heteromorphus and *Helicosphaera ampliaperta* are present in 23 of the 28 sediment samples taken from the Site 1253 cores (Table T1). Nannofossils are not present in the other five samples. The cooccurrence of these two index fossils and the absence of *Sphenolithus belemnos* and older biostratigraphic marker fossils in the sedimentary units both above and below the upper gabbro sill indicates that the entire sedimentary sequence penetrated at Site 1253 can be assigned to Martini's (1971) nannofossil Zone NN4, which corresponds to a minimum age of 15.6 Ma and maximum age of 18.2 Ma (Berggren et al., 1995b). Nannofossil Zone NN4 spans the early/middle Miocene boundary.

Site 1254

The distribution, abundance, and preservation of calcareous nannofossils recovered from Hole 1254A, correlated to the nannofossil zonation scheme of Martini (1971) and the chronologic scale of Berggren et al. (1995a, 1995b), are presented in Table T2.

Hole 1254A is located ~15 m west of Hole 1040C on the lower trench slope wedge and ~1.6 m upgradient from the toe of the slope. Coring operations at Site 1254 had two target intervals: (1) a fault zone within the prism sediments and (2) the décollement (Morris, Villinger, Klaus, et al., 2003). Sediment coring was initiated only after drilling and washing from the seafloor to ~150 mbsf, where the first target, a region of fractured sediment and locally steep bedding dips, was located (referred to as the prism fault zone). The fault zone was cored from 150 mbsf to the base of the fault zone at 230 mbsf. Below this zone, ~70 m was drilled and washed until the next target, the décollement, was reached at 300 mbsf. Coring was once again initiated, and the décollement was cored between 300 and 367.5 mbsf, where drilling and coring operations were terminated. Core recovery in these intervals averaged 88% with good hole conditions (Morris, Villinger, Klaus, et al., 2003).

Similar to the prism sediments at Site 1040 (Muza, 2000), age dating of the Site 1254 sediments is hampered by sparse abundances of nannofossils and a lithology (Fig. **F5**) suggesting that the predominant mode of sedimentation throughout the section has been gravity and debris flows (Kimura, Silver, Blum, et al., 1997; Morris, Villinger, Klaus, et al., 2003), which tend to periodically mix and introduce reworked fossils into the site of deposition. In addition, the low concentration of biogenic components (always <5%) and the abundance of quartz, feldspar, and biotite observed everywhere throughout the section leaves little doubt as to the terrigenous properties of the prism.

Compared to the same depth interval cored in Hole 1040C, the nannofossil assemblages in samples from Hole 1254A are somewhat more diverse and generally an order of magnitude (R–F) more abundant, especially between ~151 and 222 mbsf within the fault zone and from ~351 to 359 mbsf directly above the underthrust unit.

Several Pleistocene and Pliocene calcareous nannofossil marker species are present in samples from Hole 1254A, but their ranges are very sporadic, and a precise nannofossil zonation for Site 1254 is not possible. However, the tops of these marker species occur downsection in an order that does not conflict with the range of the observed marker species or the normal superposition of the sediment layers. A tentative biostratigraphy can be applied to the prism sediments at Site 1254.

The top of *Discoaster brouweri* occurs at 161.96 mbsf in Section 205-1254A-2R-5 (Table **F2**). Although *D. brouweri* is recorded farther upsection in several intervals, these occurrences represent observations of *D. brouweri* fragments within assemblages dominated by *Pseudoemiliania lacunosa* and are considered to be reworked. The extinction of *D. brouweri* occurs at 1.95 Ma, very close to the Pleistocene/Pliocene boundary.

The top of *Discoaster pentaradiatus* may occur in Section 205-1254A-5R-4 at 189.41 mbsf (several broken specimens in one isolated sample), or in Section 7R-2 at 205.97 mbsf, where whole specimens occur, albeit rarely, but are also present in Section 7R-3 at 207.15 mbsf (Table **T2**). *D. pentaradiatus* also occurs in greater numbers at ~219 mbsf, but is not suggested as the top for the species because it occurs with two other very reliable marker species (co-occurrence of *Reticulofenestra pseudoumbilica* and *Sphenolithus* spp.), implying that this sample is ~1 m.y. older. Thus, it is reasonable to suggest that the top of *D. pentaradiatus* may be either one of the intervals farther upsection (205.97 mbsf or 189.41 mbsf, the depth chosen as the top for this report). The extinction of *D. pentaradiatus* occurs at 2.55 Ma, close to the Matuyama/Gauss boundary (Berggren et al., 1995b).

The co-occurrence of abundant *R. pseudoumbilica* and *Sphenolithus* spp. in three successive samples taken at 219.14, 220.64, and 221.93 mbsf in Sections 205-1254A-8R-5, 6, and 7 indicates that this interval is no younger than 3.75 Ma. These species occur in samples that are graded "good" preservation and "abundant" in quantity along with a diverse assemblage that shows no evidence of reworking (Table T2). Unfortunately, coring was halted after recovering Core 205-1254A-8R, and 70 m of sediment was rotary drilled to ~300 mbsf before coring was resumed. *R. pseudoumbilica* and/or *Sphenolithus* spp. are also present at 351–359.81 mbsf, from Section 205-1254A-14R-4 to Section 15R-2, from 23 m below the upper boundary of the décollement to right above the base of the underthrust lithologic Subunit U1A. However, both species are long ranging, and their occurrence at that level would not be unusual. Sediments below Subunit U1A (Sections 205-1254A-15R-4 to 16R-4; from 363.65 to 367.07 mbsf; the lowest sample taken) are rich with Pleistocene diatoms. However, only the sample from 363.8 mbsf contains calcareous nannofossils. No relevant age can be deduced from this nannofossil assemblage (Table T2).

Based on the observed tops of *D. brouweri*, *D. pentaradiatus,* and *R. pseudoumbilica* in the upper cored interval at Site 1254 (150–222 mbsf), an age vs. depth plot is constructed, and possible final sediment accumulation rates are calculated for most of the represented sedimentary column (Fig. F9). Sediment may have accumulated at a rate of ~48 m/m.y. between 150 and 189.41 mbsf and ~25 m/m.y. between 189.41 and 219.14 mbsf.

F9. Age vs. depth, p. 21.

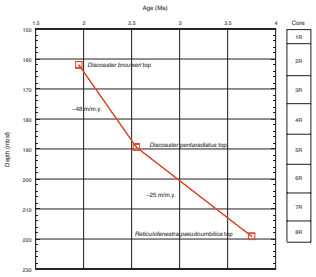

Site 1255

The distribution, abundance, and preservation of calcareous nannofossils recovered from Hole 1255A, correlated to the nannofossil zonation scheme of Martini (1971) and the chronologic scale of Berggren et al. (1995a, 1995b), are presented in Table T3.

Hole 1255A is located ~0.4 km arcward from the deformation front on the overriding plate, ~20 m east of Hole 1043A. The primary goal at this site was to identify the décollement zone, while drilling and coring, by observing anomalies in the geochemistry and penetration rates of the sediments. Successful emplacement of a long-term borehole observatory will continue to monitor the geochemistry, fluid flow, and physical parameters. Limited time at the site allowed for the recovery of only four cores. Cores were taken from 123 to 157 mbsf with 21% recovery. There was no recovery of sediments from Core 205-1255A-1R (from 123 to 132.7 mbsf).

Whole-round pore water analyses on recovered sediment further reduced the amount of core available for age dating and other studies. All of the limited amount of sediment recovered from Hole 1255A (Core 205-1255A-4R) was taken for whole-round analyses. However, coring recovered overriding plate toe sediments, as well as underthrust sediments (Fig. F6). The décollement is placed at 144.08 mbsf (Morris, Villinger, Klaus, et al., 2003).

Because of the poor core recovery and whole-round analyses, only six samples were available for biostratigraphic determination. In the top two samples from the cored sequence, taken from 133.54 and 134.67 mbsf (Section 205-1255A-2R-1), *Gephyrocapsa oceanica* and *Gephyrocapsa caribbeanica* are abundant. The absence of Pliocene species, early Pleistocene marker species such as *Helicosphaera sellii* or *Calcidiscus macintyrei*, and middle Pleistocene marker species *P. lacunosa* in these two

samples may indicate that this level is late Pleistocene in age and may even be younger than 0.46 Ma.

Interestingly, the sample taken at 142.7 mbsf (Table T3) has a characteristic assemblage nearly identical to the early Pliocene assemblages observed in Hole 1254A at ~220 mbsf in the prism sediments (Table T2).

The next lower sample in the sequence at Site 1255, taken from 144.2 mbsf, 12 cm below the décollement boundary (Table T3), is barren of calcareous nannofossils but does contain a Pleistocene diatom assemblage. An additional sample taken from 145.38 mbsf is nearly identical to the Pleistocene samples at 133.54 and 134.67 mbsf. There are no calcareous nannofossils present in the sample taken from 152 mbsf at this site; however, there are abundant diatoms present.

SUMMARY

The success of Leg 170 led to the return of the *JOIDES Resolution* to the Costa Rica subduction factory to expand upon the research generated by the Leg 170 science and further elucidate the fate of subducted materials along the Costa Rica subduction margin. Because Leg 205 drilling operations were conducted within meters of the Leg 170 drill sites, minimal coring was done during Leg 205. Although the biostratigraphy of the Leg 170 sites has been documented in detail, key questions still remained that accurate biostratigraphy could help resolve. Thus, the focus of one study centered on a gabbro sill that was only partially penetrated by coring during Leg 170. This sill was fully cored and penetrated at Site 1253 during Leg 205 along with an additional 12 m of underlying carbonate sediments and ~160 m of gabbro before coring finally was halted at 600 mbsf. Calcareous nannofossil age dating of the sediments immediately above the igneous sill, as well as the sediment between the sill and the lower igneous unit, indicates a minimum age of 15.6 Ma and a maximum age of 18.2 Ma for the sediments. This implies igneous activity younger than 18.2 Ma at Site 1253. The calcareous nannofossil assemblage in baked sediments in near-contact with the top of the lower igneous unit also suggests that the maximum age for emplacement is 18.2 Ma.

At Site 1254, coring was conducted between ~150 and 230 mbsf (prism section) and from 300 to 367.5 mbsf (prism and through the décollement into the underthrust section). Although hampered by sparse abundances and varied preservation characteristics, biostratigraphic analysis of calcareous nannofossils suggests that the sediments are early Pleistocene in age between ~150 and 161 mbsf, late Pliocene in age from ~161 to 219 mbsf, and early Pliocene in age from ~219 to 222 mbsf (no younger than 3.75 Ma). The lack of marker fossils in the interval of sediments cored from ~300 to 350.6 mbsf does not allow for any age determinations. Sediments from 351.6 to 359.81 are also early Pliocene in age and no younger than 3.75 Ma.

Only ~7.8 m of sediment was obtained from cores at Site 1255 while attempting to core through the décollement zone. Calcareous nannofossil assemblages in the upper ~2 m and lower ~2 m of sediment suggest that these sediments may be tentatively considered Pleistocene in age, and perhaps younger than 0.46 Ma.

ACKNOWLEDGMENTS

I would like to thank Julie Morris, Leg 205 Co-Chief Scientist, and members of the Leg 205 scientific party for making this research possible. Jason Chipps assisted in figure preparation. This paper benefitted from reviews by Adam Klaus and Bryan Ladner. This research used samples and/or data provided by the Ocean Drilling Program (ODP). ODP is sponsored by the U.S. National Science Foundation (NSF) and participating countries under management of Joint Oceanographic Institutions (JOI), Inc. Funding for this research was provided by a JOI-U.S. Science Support Program (USSSP) grant.

REFERENCES

Barckhausen, U., Ranero, C.R., von Huene, R., Cande, S.C., and Roeser, H.A., 2001. Revised tectonic boundaries in the Cocos plate off Costa Rica: implications for the segmentation of the convergent margin and for plate tectonic models. *J. Geophys. Res.*, 106:19207–19220. **doi:10.1029/2001JB000238**

Berggren, W.A., Hilgen, F.J., Langereis, C.G., Kent, D.V., Obradovich, J.D., Raffi, I., Raymo, M.E., and Shackleton, N.J., 1995a. Late Neogene chronology: new perspectives in high-resolution stratigraphy. *Geol. Soc. Am. Bull.,* 107:1272–1287. **doi:10.1130/0016-7606(1995)107<1272:LNCNPI>2.3.CO;2**

Berggren, W.A., Kent, D.V., Swisher, C.C., III, and Aubry, M.-P., 1995b. A revised Cenozoic geochronology and chronostratigraphy. *In* Berggren, W.A., Kent, D.V., Aubry, M.-P., and Hardenbol, J. (Eds.), *Geochronology, Time Scales and Global Stratigraphic Correlation*. Spec. Publ.—SEPM (Soc. Sediment. Geol.), 54:129–212.

Bukry, D., 1973. Low-latitude coccolith biostratigraphic zonation. *In* Edgar, N.T., Saunders, J.B., et al., *Init. Repts. DSDP,* 15: Washington (U.S. Govt. Printing Office), 685–703.

Bukry, D., 1975. Coccolith and silicoflagellate stratigraphy, northwestern Pacific Ocean, Deep Sea Drilling Project Leg 32. *In* Larson, R.L., Moberly, R., et al., *Init. Repts. DSDP,* 32: Washington (U.S. Govt. Printing Office), 677–701.

Kimura, G., Silver, E.A., Blum, P., et al., 1997. *Proc. ODP, Init. Repts.,* 170: College Station, TX (Ocean Drilling Program). [**HTML**]

Martini, E., 1971. Standard Tertiary and Quaternary calcareous nannoplankton zonation. *In* Farinacci, A. (Ed.), *Proc. 2nd Int. Conf. Planktonic Microfossils Roma:* Rome (Ed. Tecnosci.), 2:739–785.

Morris, J.D., Villinger, H.W., Klaus, A., et al., 2003. *Proc. ODP, Init. Repts.,* 205 [CD-ROM]. Available from: Ocean Drilling Program, Texas A&M University, College Station TX 77845-9547, USA. [**HTML**]

Muza, J.P., 2000. Calcareous nannofossil biostratigraphy from a 15-km transect (Cocos plate to Caribbean plate) across the Middle America Trench, Nicoya Peninsula, Costa Rica. *In* Silver, E.A., Kimura, G., Blum, P., and Shipley, T.H. (Eds.), *Proc. ODP, Sci. Results,* 170 [Online]. Available from World Wide Web: <**http://www-odp.tamu.edu/publications/170_SR/chap_05/chap_05.htm**>. [Cited 2005-05-03]

Okada, H., and Bukry, D., 1980. Supplementary modification and introduction of code numbers to the low-latitude coccolith biostratigraphic zonation (Bukry, 1973; 1975). *Mar. Micropaleontol.,* 5:321–325. **doi:10.1016/0377-8398(80)90016-X**

Perch-Nielsen, K., 1985. Cenozoic calcareous nannofossils. *In* Bolli, H.M., Saunders, J.B., and Perch-Nielsen, K. (Eds.), *Plankton Stratigraphy:* Cambridge (Cambridge Univ. Press), 427–554.

APPENDIX

Species list in alphabetical order of species epithets

Sphenolithus abies Deflandre in Deflandre and Fert (1954)
Helicosphaera ampliaperta Bramlette and Wilcoxon (1967)
Gephyrocapsa aperta Kamptner (1963)
Discoaster brouweri Tan (1927) emend. Bramlette and Riedel (1954)
Gephyrocapsa caribbeanica Boudreaux and Hay (1969)
Helicosphaera carteri (Wallich, 1877) Kamptner (1954)
Discoaster deflandrei Bramlette and Riedel (1954)
Pontosphaera discopora Schiller (1925)
Discoaster exilis Martini and Bramlette (1963)
Cyclicargolithus floridanus (Roth and Hay in Hay et al., 1967) Bukry (1971a)
Sphenolithus heteromorphus Deflandre (1953)
Pseudoemiliania lacunosa (Kamptner, 1963) Gartner (1969c)
Calcidiscus leptoporus (Murray and Blackman, 1898) Loeblich and Tappan (1978)
Discoaster loeblichii Bukry (1971a)
Calcidiscus macintyrei (Bukry and Bramlette, 1969b) Loeblich and Tappan (1978)
Reticulofenestra minuta Roth (1970)
Coccolithus miopelagicus Bukry (1971a)
Sphenolithus moriformis (Bronnimann and Stradner, 1960) Bramlette and Wilcoxon (1967)
Pontosphaera multipora (Kamptner, 1948) Roth (1970)
Sphenolithus neoabies Bukry and Bramlette (1969a)
Coronocyclus nitescens (Kamptner, 1963) Bramlette and Wilcoxon (1967)
Gephyrocapsa oceanica Kamptner (1943)
Coccolithus pelagicus (Wallich, 1877) Schiller (1930)
Discoaster pentaradiatus Tan (1927) emend. Bramlette and Riedel (1954)
Reticulofenestra pseudoumbilica (Gartner, 1967) Gartner (1969c)
Helicosphaera sellii Bukry and Bramlette (1969b)
Gephyrocapsa sinuosa Hay and Beaudry (1973)
Discoaster surculus Martini and Bramlette (1963)
Discoaster variabilis Martini and Bramlette (1963) (epithets from Perch-Nielson, 1985)

Figure F1. Bathymetry and topography of the "Costa Rica subduction factory." Leg 205 operations area is within the white bordered box (shown in more detail in Fig. F3, p. 15). Map is from Morris, Villinger, Klaus, et al. (2003).

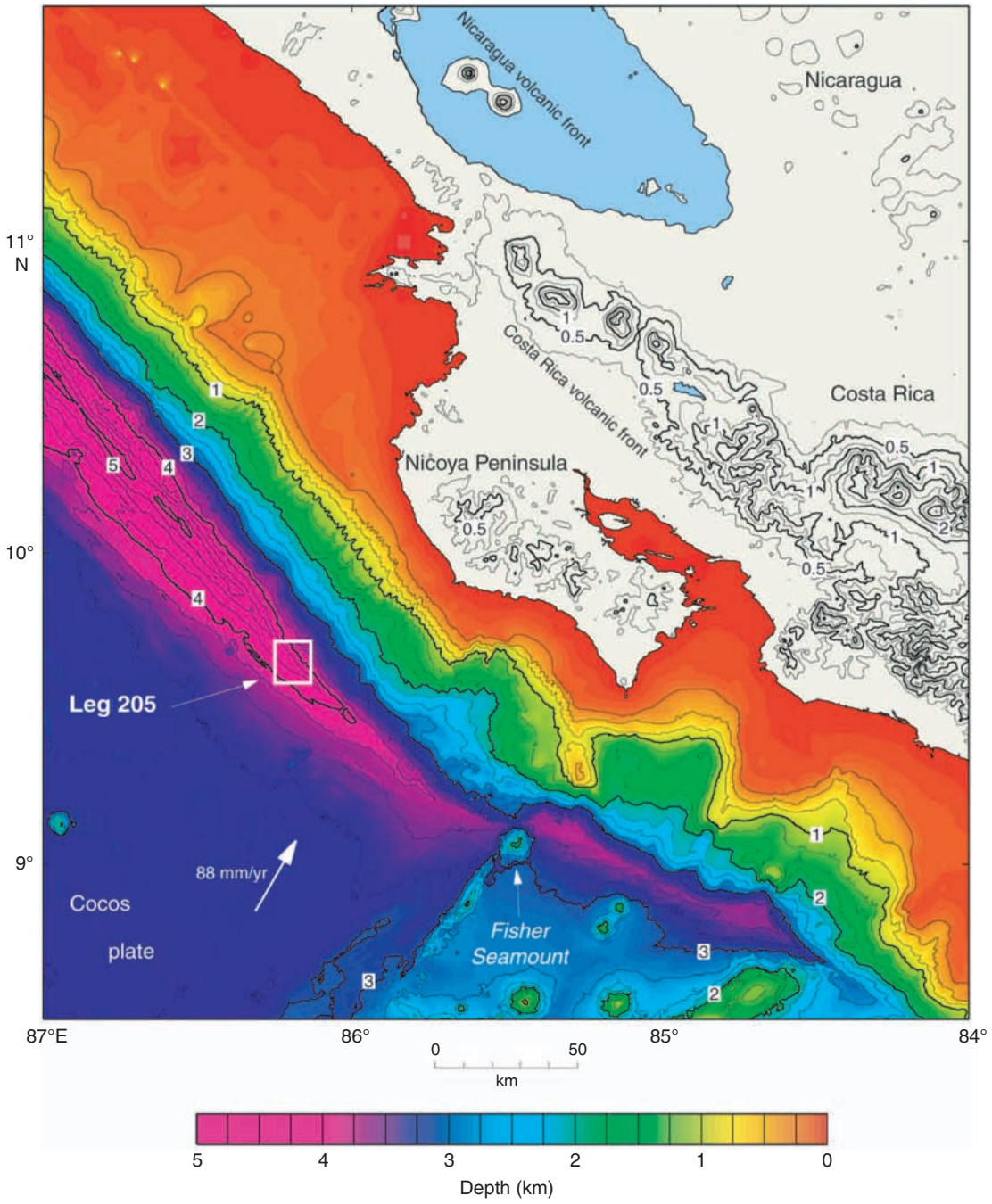

Figure F2. Leg 205 site locations along multichannel seismic Profile BGR-99-44 across the Middle America Trench. Red lines are Site 1253, 1254, and 1255 locations and depths. Black lines are locations and depths of Sites 1039, 1040, and 1043. CMP = common midpoint. Map is from Morris, Villinger, Klaus, et al. (2003).

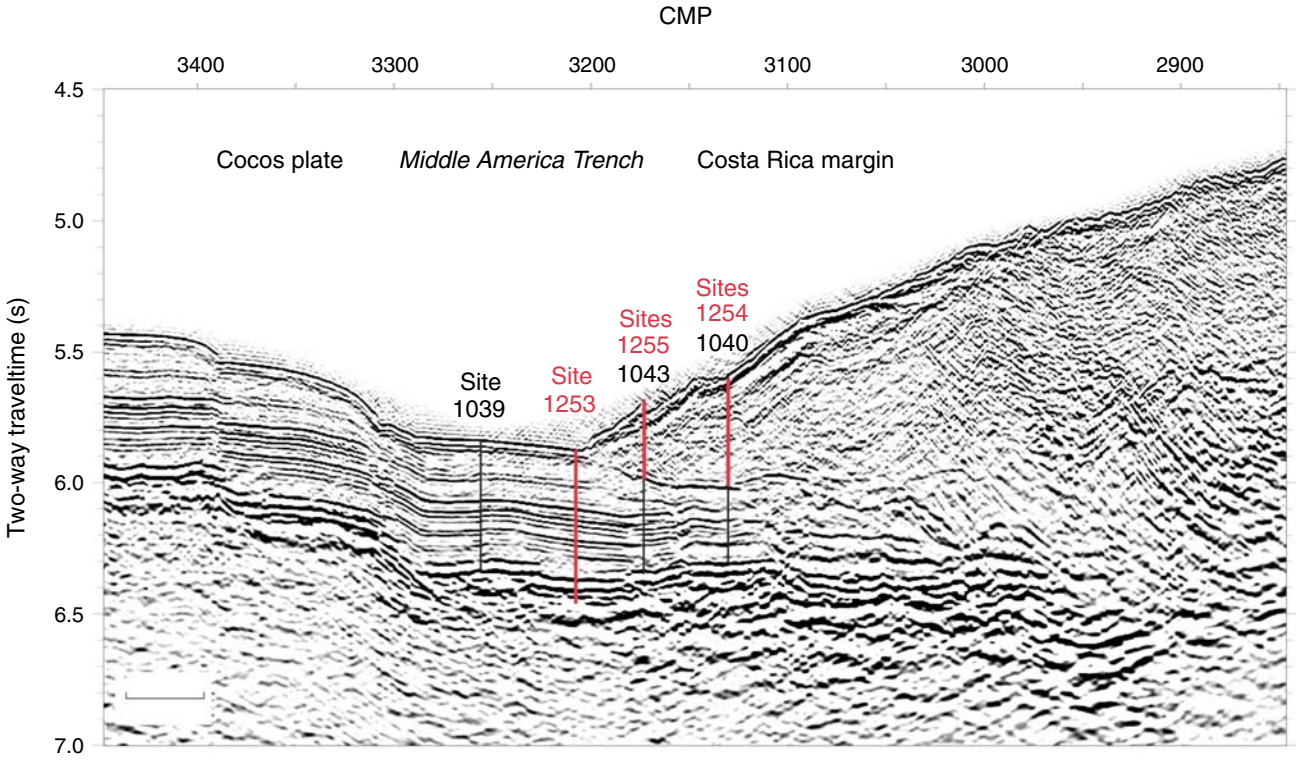

Figure F3. Bathymetric map of Leg 205 area of operations. Yellow circles are Leg 205 drill sites. Smaller white circles are Leg 170 drill sites. Red and yellow lines are seismic reflection Profiles BGR-99-44 and CR-20, respectively. Numbers along seismic lines are shotpoints, and the number with the arrow is an indication of convergence rate. Contours are in meters. The location of this site is outlined by the white box in Figure F1, p. 13. Map is from Morris, Villinger, Klaus, et al. (2003).

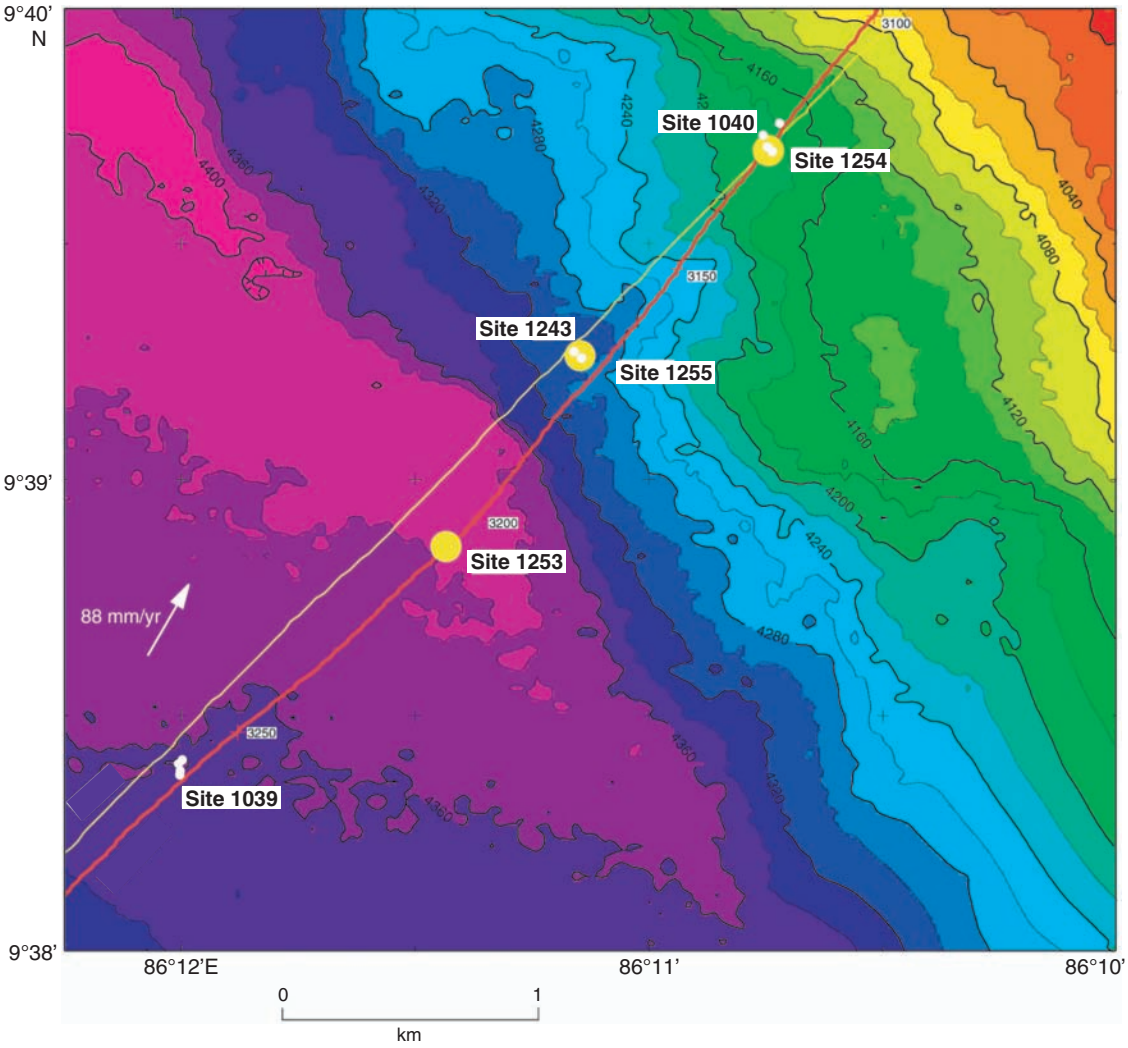

Figure F4. Stratigraphic profile of Hole 1253A correlated to the stratigraphic profiles of Holes 1039A, 1039B, and 1039C. Profile is modified after Morris, Villinger, Klaus, et al. (2003). U = underthrust units.

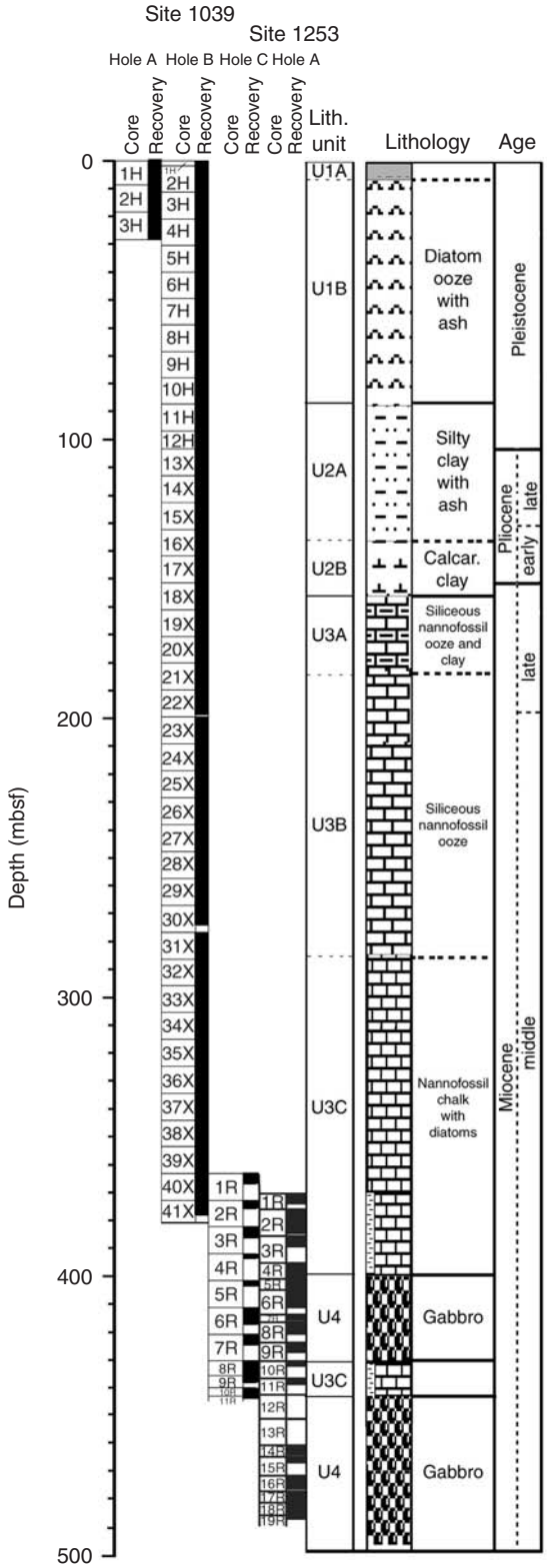

Figure F5. Stratigraphic profile of Hole 1254A correlated to the stratigraphic profile of Hole 1040C. Profile is modified after Morris, Villinger, Klaus, et al. (2003). U = underthrust units, P = prism sediments.

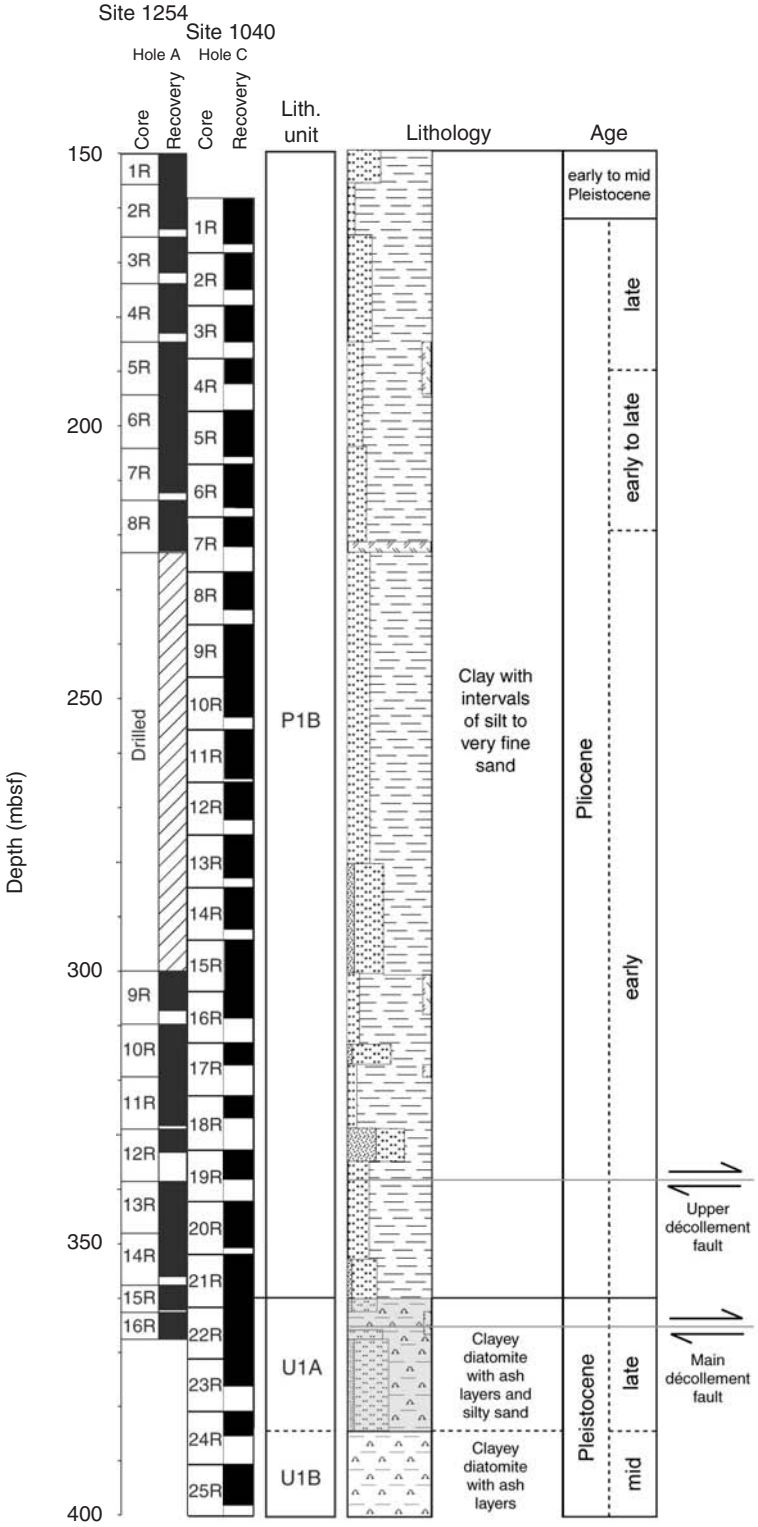

Figure F6. Stratigraphic profile of Hole 1255A correlated to the stratigraphic profile of Hole 1043A. Profile is modified after Morris, Villinger, Klaus, et al. (2003). U = underthrust units, T = toe sediments.

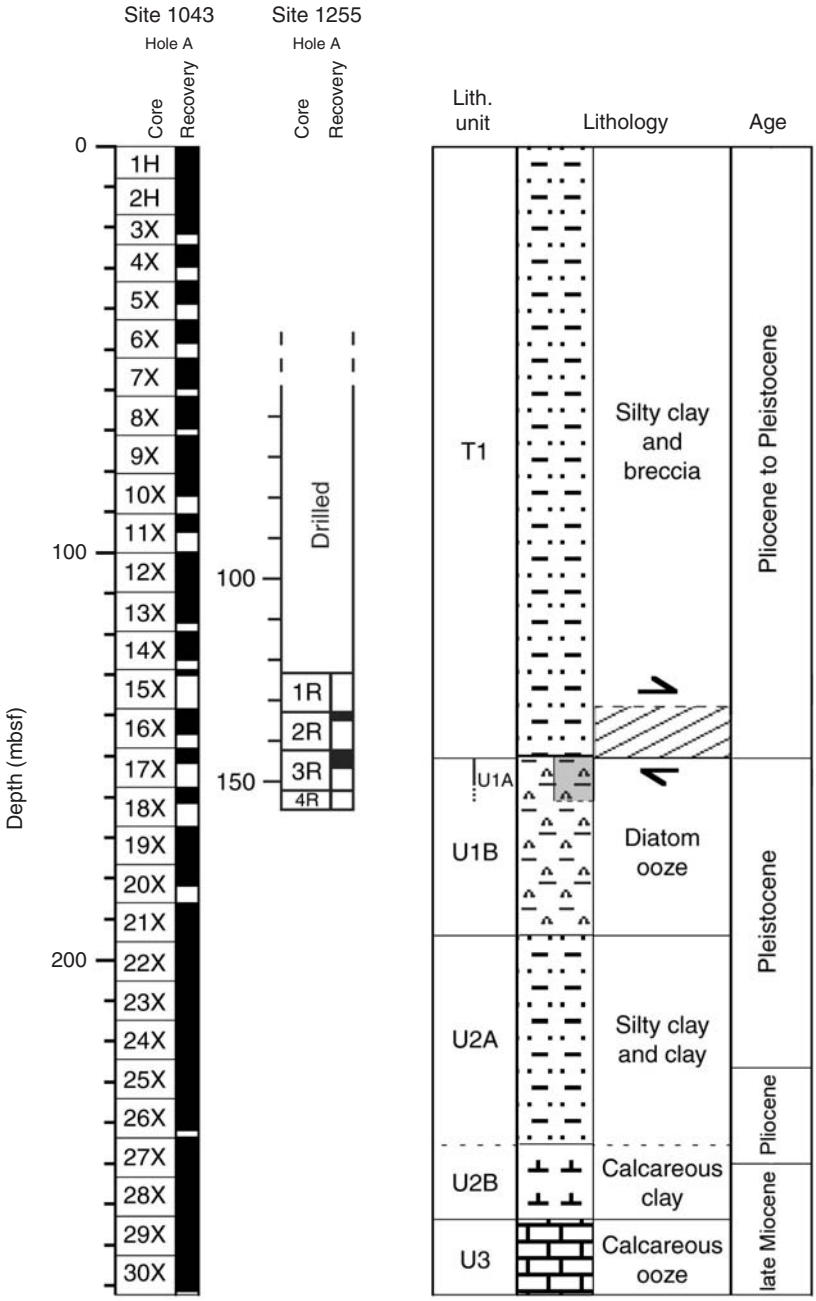

Figure F7. Geologic timescale illustrating comprehensive correlation between nannofossil zones of Martini (1971) and Bukry (1973, 1975) used in this study and the astronomical/geomagnetically derived chronologic scale of Berggren et al. (1995a, 1995b) for the Pleistocene and Pliocene.

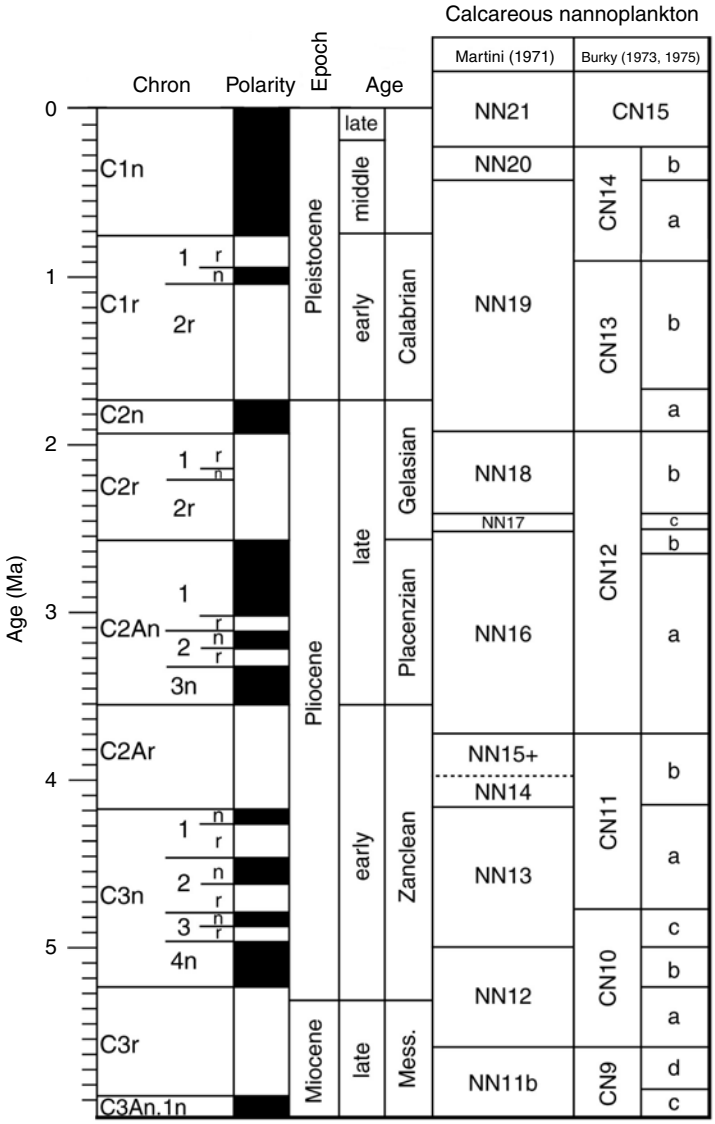

Figure F8. Geologic timescale illustrating the comprehensive correlation between the nannofossil zones of Martini (1971) and Bukry (1973, 1975) used in this study and the astronomical/geomagnetically derived chronologic scale of Berggren et al. (1995b) for the Miocene.

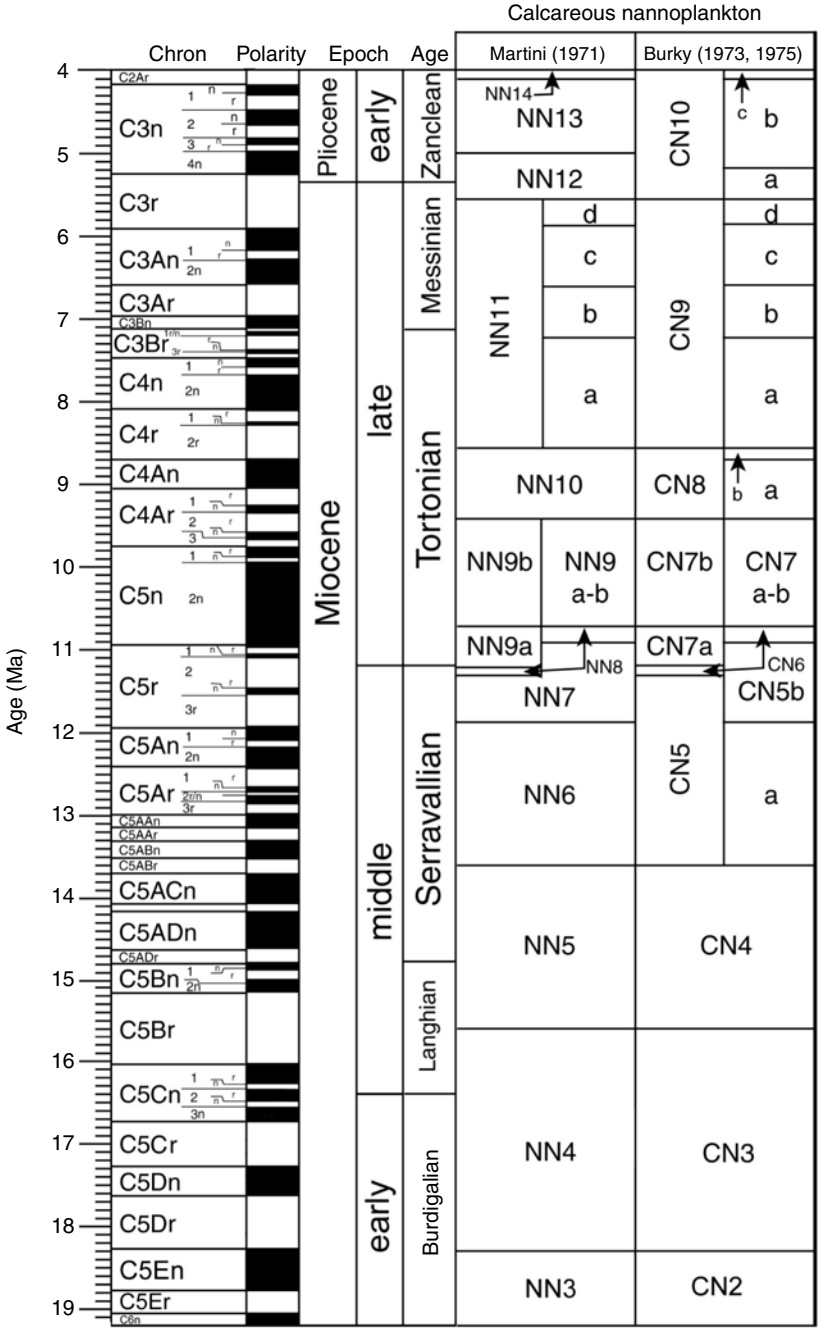

Figure F9. Biostratigraphic age vs. depth plot for Hole 1254A prism sediments. Sediment accumulation rates (m/m.y.) are calculated between the observed tops of key calcareous nannofossil species and plotted with respect to Cores 205-1254A-1R through 8R.

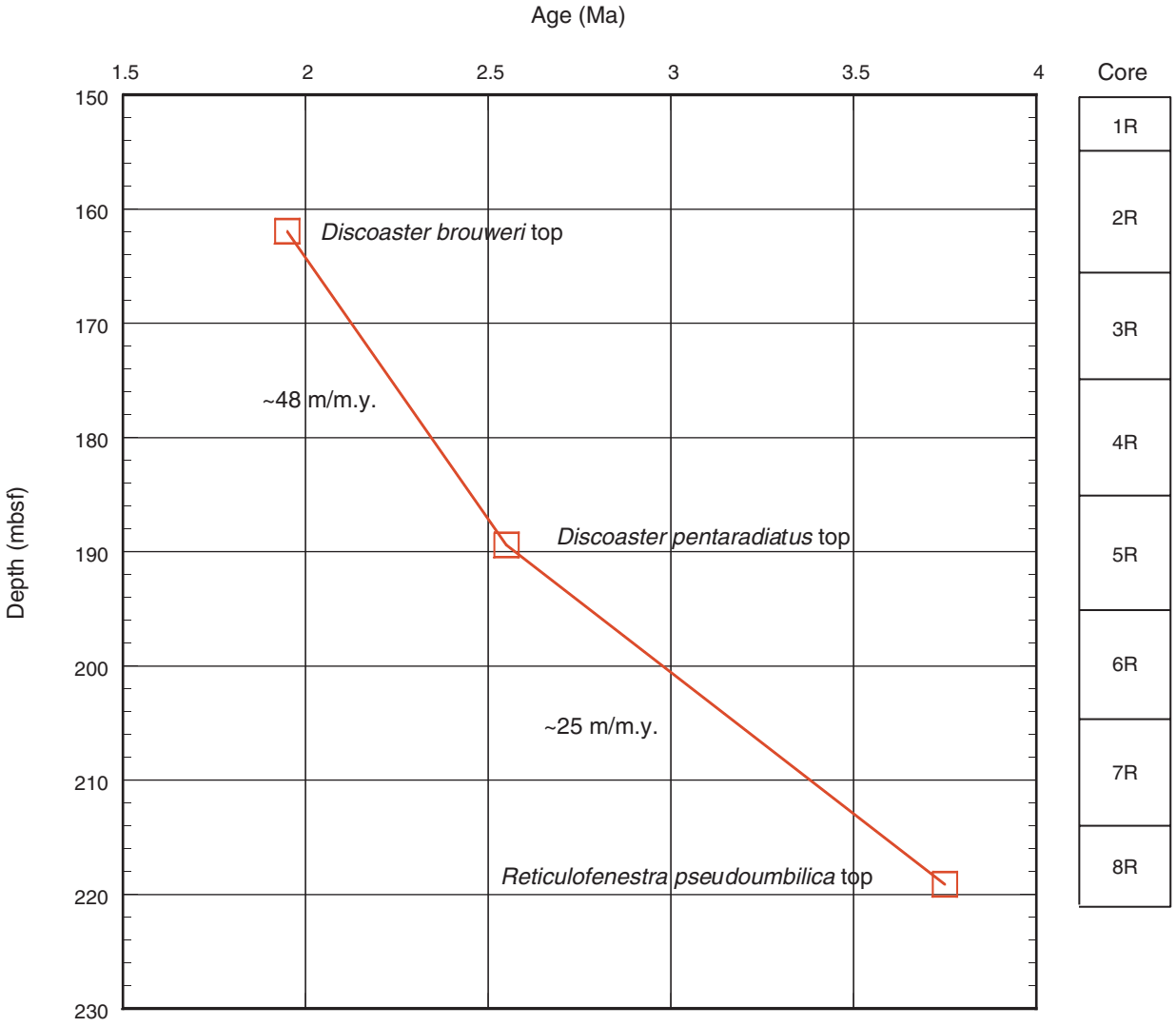

Table T1. Calcareous nannofossil range-distribution and zonation, Hole 1253A.

Core, section, interval (cm)	Depth (mbsf)	Abundance	Preservation	*Calcidiscus leptoporus*	*Coccolithus miopelagicus*	*Coccolithus pelagicus*	*Coronocyclus nitescens*	*Cyclicargolithus floridanus*	*Discoaster deflandrei*	*Discoaster druggi*	*Discoaster exilis*	*Discoaster variabilis*	*Helicosphaera ampliaperta*	*Helicosphaera carteri*	*Helicosphaera sellii*	*Pontosphaera multipora*	*Reticulofenestra minuta/minutula/haqii*	*Reticulofenestra pseudoumbilica*	*Sphenolithus abies/neoabies/moriformis*	*Sphenolithus heteromorphus*
205-1253A-																				
1C-1, 40–42	370.4	VA	G	F	A	A	C	A	C	F			F	C			A	A	A	A
1C-2, 45–47	371.81	VA	G	F	A	A	C	A	C	F	F	C	F	C		C	A	A	A	A
1C-3, 53–54	373.39	VA	G	F	A	A	C	A	C		C	C	F	A		F	A	A	A	A
2C-1, 14–15	375.74	VA	G	F	A	A	C	A	C		C	C	F	A		R	A	A	A	A
2C-2, 33–35	377.43	VA	G	F	A	A	C	A	C		C	C	F	A			A	A	A	A
2C-3, 27–28	378.41	VA	G	F	A	A	C	A	C		C	C	F	A		R	A	A	A	A
2C-4, 139–140	381.03	VA	G	F	A	A	A	A	C		C	C	F	A		C	A	A	A	A
2C-5, 72–74	381.86	VA	G	F	A	A	A	A	C		C	C	F	A		C	A	A	A	C
2C-6, 68–70	383.32	VA	G	F	A	A	C	A	A		C	C	F	A		C	A	A	A	C
2C-7, 45–47	384.09	VA	G	F	A	A	C	A	A		C	C	C	A		F	A	A	A	C
3C-1, 53–55	385.73	VA	G	F	VA	VA	C	A	A		C	C	C	A		F	A	VA	A	A
3C-2, 84–85	387.54	VA	G	F	VA	VA	A	A	A		C	C	C	C		R	A	VA	A	C
3C-3, 41–43	388.61	VA	G	F	VA	VA	A	A	A		C	C	A	C		R	A	VA	A	C
3C-CC, 12–14	389.18	VA	M	F	A	A	A	C	C		C	F	F	C			C	A	VA	C
4C-3, 40–42	398.3	B																		
4C-4, 36–37	399.46	B																		
4C-4, 84–84	399.94	B																		
Cores 4R-5 to 10R-2 are igneous.	399.95–430.72																			
10A-2, 5–6	430.77	B																		
10A-2, 18–19	430.9	B																		
10A-2, 55–56	431.27	A	P		A	C		C											C	
10A-2, 121–122	431.93	VA	M	R	A	C		A	A			F	F	C			C	A	A	A
11A-1, 0–2	436.1	VA	M		A	C		A	A				C	A			C	A	A	A
11A-1, 37–38	436.47	VA	M		A	A	C	A	C				C	A		F	C	VA	A	A
11A-1, 81–82	436.91	VA	G	F	A	A	C	A	C				A	C		F	C	VA	A	A
11A-2, 9–10	437.15	VA	G		A	A		A	C				C	A			A	VA	VA	A
11A-2, 61–62	437.67	VA	M	F	A	A		A	C				A	C			C	A	A	A
11A-2, 104–105	438.1	VA	P		C	A		A	C				C	F			A	VA	A	VA
12A-1, 18–19	442.18	VA	M	F	A	A	A	VA	A				C	C			A	VA	VA	A

Notes: Abundance: VA = very abundant, A = abundant, C = common, F = few, R = rare, B = barren. Preservation: P = poor, M = moderate, G = good.

Table T2. Calcareous nannofossil range-distribution and zonation, Hole 1254A. (**See table notes.** Continued on next page.)

Core, section, interval (cm)	Depth (mbsf)	Abundance	Preservation	*Calcidiscus leptoporus*	*Calcidiscus macintyrei*	*Coccolithus pelagicus*	*Coronocyclus nitescens*	*Discoaster brouweri*	*Discoaster pentaradiatus*	*Discoaster surculus*	*Helicosphaera carteri*	*Helicosphaera sellii*	*Pontosphaera multipora*	*Pseudoemiliania lacunosa*	*Reticulofenestra minuta/minutula/haqii*	*Reticulofenestra pseudoumbilica*	*Sphenolithus abies/neoabies/moriformis*	Unidentifiable 6-rayed discoasters
205-1254A-																		
1C-1, 132–134	151.32																	
1C-2, 33–35	151.83	C	M			F		R			F		R	F	F			F
1C-2, 33–35	151.83																	
1C-3, 39–41	153.39	C	M					R						R	F			
1C-4, 67–69	154.54							R										
1C-5, 67–69	155.54	C	M					R						R	C			F
2C-1, 134–136	156.84	C	F					R						F				
2C-2, 57–59	157.57	B																
2C-3, 84–86	159.34	C	M	F							F			F	F			R
2C-4, 71–73	160.71	F	M	R	R	R		R			R			F	F			
2C-5, 36–38	161.96	F	P			R		R							R			
3C-1, 44–46	165.54	F	M	R				R							F			
3C-2, 45–47	167.05	F	M					R			R			R	F			
3C-3, 45–47	168.55	F	M					R							F			
3C-4, 54–56	170.29	R	P					R							R			
3C-5, 27–29	171.38	R	P			R									R			
4C-1, 21–23	174.91	R	P												R			
4C-2, 23–25	176.39	B																
4C-3, 31–33	177.97	R	M	R				R							R			
4C-4, 135–137	180.51	R	M	F														R
4C-5, 18–20	180.84	R	G					R						R	F			R
4C-6, 103–105	182.64	R	G												R			
5C-1, 71–73	185.11	F	G												F			R
5C-2, 45–47	186.35	F	M	R											F			R
5C-3, 44–46	187.84	F	M		R			R	R		R				F			
5C-4, 51–53	189.41	F	M					R							F			
5C-5, 17–19	190.07	F	M			R	R				R				F			
5C-6, 51–53	191.36	B																
6C-7, 42–44	192.77	R	G												R			
6C-1, 75–77	194.85	F	M			R		F			R	R		F	F			F
6C-2, 74–76	196.46	R	M	R								R			R			
6C-3, 74–76	198.17	F	M								R				F			
6C-4, 74–76	199.67	C	M	F	R	R		F			F	R			C			R
6C-5, 64–66	201.07	C	M					F							C			
6C-6, 59–61	202.52	B																
7C-1, 68–70	204.48	F	M						R						F			
7C-2, 67–69	205.97	F	M			R			R		R				F			R
7C-3, 35–37	207.15	R	M		R			R							R		R	
7C-4, 77–79	209.07	B																
7C-6, 38–40	210.38	F	M								R				F			
7C-7, 37–39	211.57	B																
8C-1, 99–101	214.39	B																
8C-2, 100–102	215.9	R	M								R				R		R	
8C-3, 99–101	217.39	A	M	F				C	F	R	C				A	A	A	
8C-5, 99–102	219.14	A	M	F	F			F	F		F				A	C	A	F
8C-6, 99–101	220.64			F	F						C				A	A	C	
8C-7, 78–80	221.93																	
~70 m drilled and washed (no coring)																		
9C-2, 121–123	302.71	B																
9C-2, 144–146	302.94	F	P	R							R				F			
9C-3, 99–101	303.99	R	P	R							R				R			
9C-4, 60–62	305.1	R	P												R			
9C-6, 78–80	306.73	B																
10C-1, 132–134	311.02	F	P	F		R			R		F	R			R			
10C-2, 33–35	311.53	F	P	F							R				F			R

Table T2 (continued).

Core, section, interval (cm)	Depth (mbsf)	Abundance	Preservation	*Calcidiscus leptoporus*	*Calcidiscus macintyrei*	*Coccolithus pelagicus*	*Coronocyclus nitescens*	*Discoaster brouweri*	*Discoaster pentaradiatus*	*Discoaster surculus*	*Helicosphaera carteri*	*Helicosphaera sellii*	*Pontosphaera multipora*	*Pseudoemiliania lacunosa*	*Reticulofenestra minuta/minutula/haqii*	*Reticulofenestra pseudoumbilica*	*Sphenolithus abies/neoabies/moriformis*	Unidentifiable 6-rayed discoasters
10C-3, 48–50	313.18	C	G												C			R
10C-4, 94–96	315.14	C	M	R											C	R		R
10C-5, 43–45	316.13	B																
10C-7, 118–119	318.36	C	P	F							R				C			R
10C-8, 49–51	319.17	C	P												C			
11C-2, 39–41	320.92	C	M								R				C			R
11C-3, 40–42	322.43	F	M	R											F			
11C-4, 67–69	324.2	F	M									F			F			F
11C-6, 40–42	326.52	F	M	R							R				F			R
11C-7, 29–31	327.91	F	M												F			
Upper boundary of décollement zone																		
13C-1, 80–82	339.3	F	M												F			
13C-2, 25–27	340.25	F	M												F			
13C-4, 93–95	343.93	F	M												F			R
13C-6, 41–43	345.55	R	M	R											R			R
13C-7, 44–46	347.08	F	G								R				F		F	
14C-1, 75–77	348.85	R	P	R														R
14C-2, 100–102	350.6	R	P												R			
14C-4, 34–36	351.6	R	M												R	R	R	
14C-5, 44–46	353.2	C	M								R				C		C	
14C-7, 31–33	355.09	R	G												R		R	
15C-1, 83–85	358.53	C	G												C	C	F	
15C-2, 61–63	359.81	C	G						R		R				C	C	C	
Hemipelagic Subunit U1A of the underthrust (lithologic [diatoms] boundary at 360.6 mbsf)																		
15C-4, 50–52	361.65																	
16C-1, 110–112	363.8	F	M	R							R				F			
Base of décollement	364.2																	
16C-2, 106–108	365.26	B																
16C-4, 43–45	367.07	B																

Notes: Abundance: A = abundant, C = common, F = few, R = rare, B = barren.
Preservation: P = poor, M = moderate, G = good.

Table T3. Calcareous nannofossil range-distribution and zonation, Hole 1255A.

Core, section, interval (cm)	Depth (mbsf)	Abundance	Preservation	*Calcidiscus leptoporus*	*Calcidiscus macintyrei*	*Coccolithus pelagicus*	*Coronocyclus nitescens*	*Discoaster brouweri*	*Gephyrocapsa caribbeanica*	*Gephyrocapsa oceanica*	*Helicosphaera carteri*	*Helicosphaera sellii*	*Pontosphaera discopora*	*Pontosphaera multipora*	*Pseudoemiliania lacunosa*	*Reticulofenestra minuta/minutula/haqii*	*Reticulofenestra pseudoumbilica*	*Sphenolithus abies/neoabies/moriformis*	Unidentifiable 6-rayed discoasters	Unidentifiable placoliths
205-1255A-																				
2C-1, 84–86	133.54	C	M	R					C	C						C				
2C-3, 25–27	134.67	A	G	R					A	A			R	R		A				
3C-1, 30–32	142.7	A	M	R	R	F		F								A	C	C	F	
3C-2, 30–32	144.2	B																		
3C-3, 15–17	145.38	A	G	F					A	A	C					A				
4C-1, 0–1	152	B																		

Notes: Abundance: A = abundant, C = common, F = few, R = rare, B = barren. Preservation: G = good, M = moderate.

Table T4. Calcareous nannofossil biostratigraphic marker species observed in Leg 170 and 205 core samples.

Index fossil	Age (Ma)
B *Emiliania huxleyi*	0.26
T *Triquetrorhabdulus rugosus*	0.46
T *Helicosphaera sellii*	1.47
T *Discoaster brouwerii*	1.95
T *Discoaster pentaradiatus*	2.55
T *Reticulofenestra pseudoumbilicus*	3.75
T *Sphenolithus abies/neoabies*	3.75
T *Triquetrorhabdulus rugosus*	5.34
T *Discoaster quinqueramus*	5.60
T *Discoaster loeblichii*	7.40
B *Discoaster berggrenii*	8.60
B *Discoaster loeblichii*	8.70
T *Discoaster hamatus*	9.40
B *Discoaster hamatus*	10.70
T *Coccolithus miopelagicus*	10.80
T *Discoaster kugleri*	11.50
B *Discoaster kugleri*	11.80
T *Cyclicargolithus floridanus*	11.80
T *Sphenolithus heteromorphus*	13.60
T *Helicosphaera ampliaperta*	15.60
B *Sphenolithus heteromorphus*	18.20

Note: Datums and ages are from Berggren et al. (1995a, 1995b).